J. Applied Membrane Science & Technology, Vol. 24, No. 1, April 2020, 11–26

Separation of Acetic Acid and Water Using Reverse Osmosis Membranes

Nora Jullok[a,b*] & Boo Chie Hang[a]

[a]School of Bioprocess Engineering, Universiti Malaysia Perlis, Kompleks Pusat Pengajian Jejawi 3, 02600, Arau, Perlis, Malaysia
[b]Centre of Excellence for Biomass Utilization, Universiti Malaysia Perlis, Kompleks Pusat Pengajian Jejawi 3, 02600, Arau, Perlis, Malaysia

Submitted: 12/7/2019. Revised edition: 16/10/2019. Accepted: 16/10/2019. Available online: 5/3/2020

ABSTRACT

Reverse osmosis can potentially be used for separation of acetic acid from waste stream. However, the investigation on the separation of this binary mixture utilizing reverse osmosis is scarce. Thus, this study aims to evaluate the feasibility of lab-synthesized and commercially available reverse osmosis membranes to separate low acetic acid concentration from aqueous mixture. A commercially available AG membrane and three laboratory synthesized polysulfone (PSf) membranes were used in this work. Initial test for water permeation using dead end filtration found that 17.5 wt% PSf has the highest water permeability. As the polymer concentration decreases, the membrane porosity increases which decreases the resistance which enables the penetration of the permeant more easily through the membrane matrix resulting in higher water permeation when 17.5wt% PSf was used. Further modification by interfacial polymerization to form a thin polyamide layer on the porous support was seen to have had improved the membrane affinity towards water resulted in increased of permeation through the membrane matrix. However, the rejection was lower than that of the AG membrane. This indicates that, the increase in water permeation when 17.5wt%PSf was used is due to the high membrane porosity. This is evidence since 17.5wt%PSf has the highest water flux but lower acetic acid rejection compared to the commercial AG membrane. Low rejection of acetic acid when reverse osmosis membrane was applied indicates that other factor such as Donnan effect has to be further considered when synthesizing the membrane.

Keywords: Polyamide, polysulfone, acetic acid separation, interfacial polymerization, reverse osmosis

1.0 INTRODUCTION

Acetic acid (HAc) is one of the light carboxylic acids (LCA) which serves as a most important raw or intermediates in the production of acetate ester, vinyl acetate monomer (VAM), acetic anhydrate synthesis and in the production of Terephthalic Acid (TPA), which is used as a solvent [1]. In a year, 6.5 million tonnes of acetic acid produced worldwide which approximately 5 million tonnes are produced by bacterial fermentation and also methanol carbonylation process meanwhile the rest 1.5 million tonnes are produced through recycling [2]. About 75% of acetic acid productions have been produced in the chemical industry via methanol carbonylation also known as Monsanto process. In Monsanto process, acetic acid was

* Corresponding to: Nora Jullok (email: norajullok@unimap.edu.my)
DOI: https://doi.org/10.11113/amst.v24n1.168

produced via reaction between methanol and carbon monoxide catalysed by rhodium complex catalyst at temperature of 180 ℃ and pressure of 30–40 atm [3].

In many industrials processes such as textile, food, pharmaceutical, paper mills, petrochemical, fine chemicals industries and semiconductor, the light carboxylic acid is produced as a by-product. This by-product generates organic acid contamination in a large water fluxes due to the oxidation reaction [4]. In these industries, there are several stages such as resist coating, deposition, and resist removal, light exposure, etching, rinsing and finishing processes in the production process of liquid crystal, semiconductor, electronic industries and textile industries which generated wastes that contains huge amount of acid wastes. For example the semiconductor of silicon wafer process uses the mixed acids to get rid of deterioration generated in wafer cutting. In electronics industry, the production of semiconductors consumes large quantities of ultra-pure water. A significant amount of polluted waste water is generated that required to be treated before discharging or re-using it for production cycle [5]. The composition of the acid waste depends on the reaction conditions of etching process in semiconductor which generally consists of 30–40% nitric acid (HNO_3), 7–12% acetic acid ($C_2H_4O_2$), 10–25% hydrofluoric acid (HF) and 1.5–2.5% silicon [6,7]. Due to the significant concentration, it is crucial to develop some alternative sources which economically viable to recover these acids prior to treatment in wastewater plant for final disposal.

There are many conventional methods have been employed for separation of acetic acid from water such as distillation [8], liquid-liquid extraction [9], adsorption [10], and precipitation [11]. Another method which usually applied to separate acetic acid and water is via pervaporation. Pervaporation is a potential method separate azeotropic and close boiling point mixture (e.g., acetic and water) [12]. However, study related to separation of organic acids in water using reverse osmosis is scarcely available. Thus, this study aims to investigate the potential of organic acids recovery from aqueous solutions, which are from the low concentrations of organic acids in industrial wastewater such as from semiconductor, textile, and in petrochemicals. In this study, the recovery of the acetic acid from aqueous mixture will be done by using reverse osmosis system.

2.0 MATERIALS AND METHODS

2.1 Material and Chemical

In the experiment four membranes were used; one commercial AG membrane from GE Osmonics™ and three laboratory-synthesized polymeric membranes. AG membrane is a polyamide flat sheet membrane. This commercial membrane needs to be immersed in water for 24 hours to remove any impurities present on the membrane active layer. Another three membranes were synthesised in the laboratory using Polysulfone (PSf) resins, purchased from Solvay Advanced Polymers Malaysia. PSf was dissolved at specific ratio with N-methyl-2-pyrrolidone (NMP, 99.5%) was purchased from Merck Sdn. Bhd. Malaysia and used as a solvent, to dissolve the PSf resins. About 2L of distilled water was filled into a basin and used as a coagulation bath. The formed film (membrane support) was further modified to produce a thin film composite (TFC) membrane via

interfacial polymerization. This reaction required, amine monomer metaphenylene diamine (MPD, 98.0%) and acid chloride monomers trimesoyl chloride (TMC, 98%), which were supplied by Merck Sdn. Bhd., Malaysia. Distilled water was used as solvent for amine monomers, meanwhile hexane which was obtained from Fisher Chemical Malaysia was used as a solvent for acid chlorides monomers. Acetic acid (HAc, 99.85%) was purchased from HmbG Chemicals Malaysia.

2.2 Membrane Synthesis

2.2.1 Preparation of Asymmetric Support Membrane Layer

An asymmetric membrane support layers were synthesised using phase inversion which was induced by immersion precipitation. This method is also known as non-solvent induced phase separation (NIPS). Other researchers had synthesized microporous support membrane using 16 to 21wt% PSf as dope solution [13, 14]. By taking the concentration of dope solution within this range polysulfone polymer at concentrations of 17.5 wt% and 20.0 wt%PSf were used and dissolved in NMP solvent by using roller 6 basic shaker at room temperature until the solution became homogenous. The film was casted on a glass plate using an Elcometer 3580 film applicator with thickness adjusted to 250 µm. The casted polymer film was immersed into a coagulation water bath at room temperature for at least 24 hours where the interchange of the solvent and non-solvent occurs to allow the phase separation of casting solution to takes place [15]. Figure 1 shows a flowchart of the membrane support fabrication and the interfacial polymerization to produce a TFC membrane.

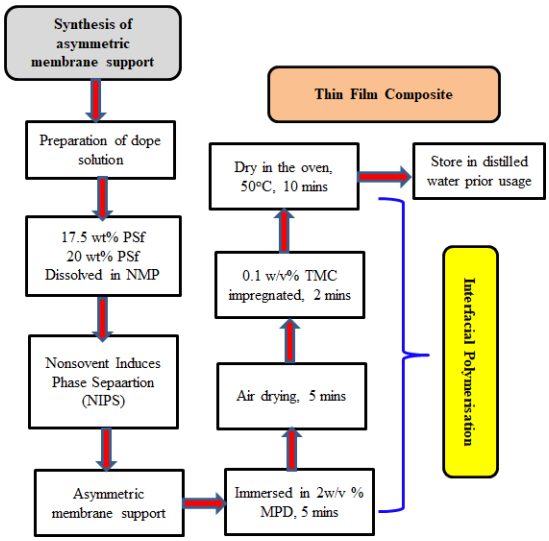

Figure 1 Synthesis route of TFC membrane

2.2.2 Preparation of Thin Film Composite Polyamide Membrane

Membrane modification, which indicated as (M) was done by interfacial polymerisation on the synthesized membrane with the highest water permeation flux. The PSf support membrane was immersed for 5 minutes in aqueous solution of MPD (2 w/v%) in water. Then the excess aqueous solution was drained off from the surface by standing the membrane holder until there was no excess of liquid remained and followed by 5 minutes air drying. The saturated surface of the membrane was then impregnated into the hexane solution of TMC (0.1 w/v%) for 2 minutes to form a thin film of polyamide layer on the top of PSf membrane support. The membrane was then placed in the oven at 50°C for 10 minutes as a post-treatment before it was stored in distilled water prior to usage [16]. The process flow diagram is as shown in Figure 1.

2.3 Reverse Osmosis Experiment

The performance of the synthesized membrane on the separation of HAc/water mixture was done by using dead end filtration HP4750 Stirred Cell, Sterlitech™ Corporation (USA). This membrane module is the simplest and the fastest when it comes for membrane testing. This experiment aims estimate the solute and solvent permeabilities and the rejection rate of the membrane. Nitrogen gas was used and regulated using pressure regulator to obtain 15, 20 and 25 bars of pressure at ambient temperature. The active membrane area was 14.6 cm^2. The feed concentrations of acetic acid solutions were varied at 10 wt%, 15 wt% and 20 wt% HAc. 250 mL of the HAc/water mixture was poured into the membrane cell and tightly sealed. The solution was continuously stirred to prevent from concentration polarization to occur. The water that permeated through the membrane matrix was collected using a measuring cylinder and recorded. The initial feed concentration and permeate concentration (final) were analysed using refractometer. The determination of the membrane permeability and rejection rate was then calculated to evaluate the membrane performances.

2.3.1 Flux and Permeability

Flux is the amount of volume of the water that passes through a membrane per unit surface area of the membranes and time. Samples were taken triplicate. The membrane flux (J) and permeability (P) were calculated using Equation 1 and Equation 2.

$$J = \frac{\Delta V}{A_m \cdot \Delta t} \quad (1)$$

$$P = \frac{J}{\Delta p} \quad (2)$$

where ΔV is the permeate volume (L), A_m is the effective membrane area (m^2), Δt is the time (h) and Δp is the difference of transmembrane pressure (bar).

2.3.3 Rejection Rate

To evaluate the rejection rate, R_{rej} (%) of acetic acid, the following Equation 3 was employed.

$$R_{rej}(\%) = \left(1 - \frac{C_P}{C_F}\right) \times 100 \quad (3)$$

where C_P is the acetic acid concentration in the permeate solution and C_F is the acetic acid concentration in the feed solution.

2.3.4 Osmotic Pressure to Solute Concentration Ratio

The osmotic pressure coefficient was determined from the correlation with feed concentration and variation of the pressure by calculation using Equation 4:

$$[\Delta p - (J_W/A_W)] = \Psi(C_F - C_{P)} \quad (4)$$

where Δp is operating pressure gradient (kg/m h^2), J_W is water flux (L/m^2 h), A_W is water permeability constant (h/m) and Ψ is osmotic pressure to solute concentration ratio (m^2/h^2).

2.4 Membrane Characterization

2.4.1 Field Emission Scanning Electron Microscopy (FESEM)

Field Emission Scanning Electron Microscope (FESEM, NOVA NANOSEM 450) measurements were used to visualize the membrane morphology. Membranes were cut into pieces of small sizes and submerged

into liquid nitrogen and fractured for cross section analysis. After that membranes were glued on a carbon tab and coated with platinum using Auto line coater (JEOL: JFC-1600) before samples were placed inside the FESEM chamber for analysis.

2.4.2 Fourier transforms Infrared Spectroscopy (FTIR)

Fourier Transform Infrared (FTIR spectrum 65, PerkinElmer) spectroscopy with attenuated total reflection (ATR) plate was used to observe the surface functional group of the membrane.

3.0 RESULTS AND DISCUSSION

3.1 Pure Water Permeability Constant

Pure water permeability constant measurement of different membranes was the main parameter which was examined for describing the membrane performance. Pure water permeability constant, A_W, was obtained from the slope of pressure vs flux data which was calculated using Equation (5) and was shown in Figure 2. The pure water flux of each membrane for pressure ranging from 15 to 25 bar was measured at room temperature. For pure water, the osmotic pressure ($\Delta\pi$) is equal to zero, thus, $A_W = J/\Delta P$ for pure water. As shown in Figure 2, the pure water permeability constant of AG, 17.5 wt% PSf, 20.0 wt% PSf and 17.5 wt% PSf (M) were 1.38, 4.49, 1.32, 1.82 L/m^2 h bar, where 17.5 wt% PSf > 17.5 wt% PSf (M) > AG > 20.0 wt% PSf. The pure water permeability constant, A_W, was used to determine the osmotic pressure to solute concentration ratio, Ψ.

$$[\Delta p - (J_W/A_W)] = \Psi(C_F - C_{P)} \quad (5)$$

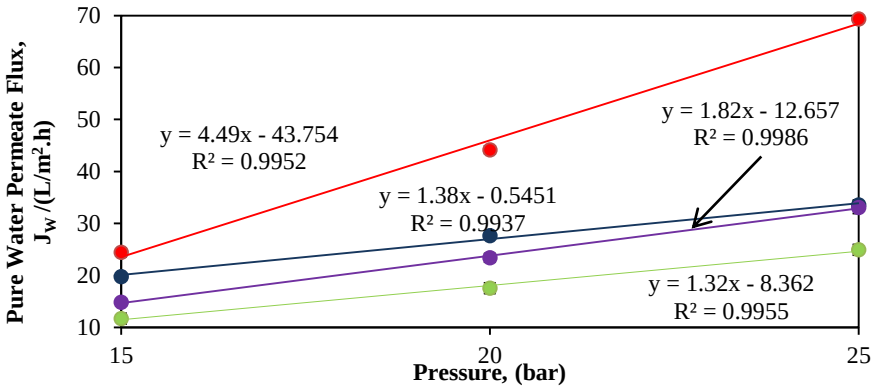

Figure 2 Pure water permeates flux of different membranes at different pressure ●AG, ● 17.5wt%PSf, ●20wt%PSf and ●17.5wt%PSf (M)

3.2 Water Permeability of Membrane

A summary of water permeabilities through the membranes in terms of per unit pressure were calculated using Equation 2 (see Table 1). From this table, it can be seen that the permeability of water decreases as the concentration of acetic acid increases in the feed solution for all the membranes. This was due to increases acetic acid concentration in the feed solution and water molecules

decreases, which may have caused the polarisation effect of acetic acid molecules, and ultimately lessen the water penetration through the membrane matrix.

Moreover, it was observed that the permeability of water was slightly increased when pressure increased. This is because, when pressure is increased, the pressure gradient increase which increases the driving force for the permeant to pass through the membrane matrix, which finally increases the flux. According to the permeability equation (Equation 2) the permeability is directly proportional to the flux; therefore increases pressure will increase the flux and indirectly increases the permeability. From Table 1, it can be seen that 17.5 wt% PSf membrane has the highest water permeability in all feed concentrations compared to membrane AG, 17.5 wt% PSf (M) and 20.0 wt% PSf. Some overlapping values of fluxes were seen when pressure was increased from 15 to 20 bar and 20 to 25 bar. It was hypothesized that the occurrence was mainly due to membrane compaction process.

Table 1 Water Permeability data of different membrane at different concentration of acetic acid solution

Acetic Acid (wt%)	Pressure (bar)	Water Permeability of Membrane (L/m^2.h.bar)			
		AG	PSf 17.5wt%	PSf 20.0 wt%	PSf (M) 17.5 wt%
0	15	1.27–1.36	1.54–1.73	0.75–0.81	0.99–1.00
	20	1.37–1.40	2.17–2.28	0.84–0.93	1.12–1.26
	25	1.27–1.39	2.73–2.79	0.98–1.03	1.26–1.42
10	15	0.17–0.19	0.93–0.99	0.36–0.38	0.54–0.60
	20	0.19-0.21	1.20–1.24	0.60–0.61	0.70–0.78
	25	0.18-0.20	1.32-1.34	0.65–0.67	0.92–1.02
15	15	0.14-0.16	0.44–0.46	0.31–0.33	0.29–0.34
	20	0.16-0.18	0.56-0.58	0.30–0.32	0.34–0.35
	25	0.16–0.17	0.60–0.64	0.33–0.34	0.38–0.39
20	15	0.11-0.13	0.31–0.33	0.14-0.16	0.22–0.23
	20	0.10-0.12	0.45–0.46	0.15-0.17	0.23–0.25
	25	0.12-0.14	0.47–0.48	0.12-0.14	0.26-0.28

3.3 Effect of Pressure and Feed Concentration on Dead End Filtration Test

In order to recover acetic acid from water mixture, the effect of operating conditions on rejection rate was also been studied. Figure 3 to 6 show the effect of pressure on the water permeation flux and rejection rate at different feed concentrations. The pressure tested in this work was varied from 15 to 25 bar and the feed concentrations of acetic acid ranged from 10 wt% HAc to 20 wt% HAc. According to Qi *et al*. (2011), changes in permeates flux caused by pressure variations also influenced the membrane fouling and concentration polarization, thereby affecting the retention of solute. The results shown in Figure 2 to 6 indicate that the permeate water flux increases linearly with increasing pressure for all the membranes. These results also signify that the membrane fouling could be neglected in applied pressure range [17]. The highest water permeability was obtained when 17.5 wt% PSf membrane was used. The AG

membrane has the lowest water permeability among all the membrane; however the rejection rate was the highest compared to the other synthesized membranes. The rejection of solute in RO is often influence by a few factors; solute, membrane properties, feed composition and operating conditions. Solute can be rejected on RO by one or combination of three basic mechanisms: size exclusion (sieving, steric effect), charge exclusion (electrical, Donnan) and physic-chemical interactions between solute, solvent and membrane [18]. Similar results was obtained when Teella *et al.* 2011, investigated on the separation of acetic acid from aqueous fraction of fast pyrolysis bio-oils using RO AG membrane, where RO AG membrane has low flux but high rejection [19].

Moreover, Figure 3 to 6 also illustrates the water permeabilities at three feed concentrations of HAc; 10.0 wt%, 15.0 wt% and 20.0 wt%. from these figures, it was observed that, the water permeability decreases as the acetic acid feed concentration increases for all the membrane tested. This is logical since the saturation of HAc molecules in the mixture may have caused the water molecules to be distanced from the membrane surface. As a consequence, the physic-chemical interaction between water/membrane was disrupted and affected the water permeation through the membrane matrix [18].

3.4 Effect of Pressure and Feed Concentration on Rejection Rate

The effect of pressure and feed concentration on the rejection rate was investigated and has been plotted into a graph and presented in Figure 3 to 6. The results indicate that the slightly increased of rejection rate of solute as pressure increases for all membrane could be explained by the solution-diffusion mechanism [20]. The increment of water adsorption into the membrane pores than acetic acid was caused by the increasing of the pressure, due to the stronger interaction of water with the hydrophilic active layer of the membrane than solute molecules (acetic acid) through hydrogen bonding [20]. Therefore water was more permeable than acetic acid, resulting high solute rejection rate. In Figure 3, it shows that, the highest rejection rate of HAc was obtained using the commercial AG membrane ranged from 20% – 26% rejection when tested in 10.0 wt% HAc and gradually decrease when the concentration of HAc in the feed solution is increased. Compared with others membranes (Figure 4 to 6), all the synthesized membranes have the overall rejection rate of less than 3% in all concentration of HAc. The commercial AG membrane has the highest rejection rate and this was due to the homogeneous thin film of polyamide layer (Figure 11(A)) on the membrane top layer. Although the 17.5 wt% PSf (M) (Figure 11(D)) membrane has undergone a modification, the thin film polyamide layer produced on the membrane surface was not homogeneously formed. This could potentially be due to the membrane that was not completely flattened during the interfacial polymerisation reaction which had caused disintegration between chemicals and membrane surface. The unevenly formation of thin film polyamide layer was seen to have had caused membrane defect and thus low rejection rate was obtained when 17.5 wt% PSf (M) membrane was applied.

In addition, Figure 3 to 6 demonstrates that the higher the HAc feed concentration, the lower the

rejection rate. The decrease of rejection rate with increase of HAc feed concentration could be due to the variations of pH in feed concentration and this could be explained by Donnan effect [21, 22]. The Donnan effect which is caused by the electrostatic interaction between transport of charged solutes molecules (acetic acid) and membrane [21, 23]. The increase of acetic acid concentration in the feed, it will decrease the pH of the feed concentration. The acetic acid molecules were in neutral form when the pH value was lower than the pKa of acetic acid. While the pH value higher than pKa, the acetic acid will start to dissociate and the sharp increment in dissociation degree as pH increase. Weng *et al*., (2009) reported that the rejection of acetic acid increased from -3% to more than 90% as the pH increases from pH 3 to pH 9, this result shows that at low pH the acetic acid tends to be neutral form and as pH increased the acetic acid was deprotonized as negatively charged acetate. At higher pH value, the thin film polyamide membrane becomes negatively charge [24]; therefore increased the electrostatic repulsion between negatively charge acetic acid molecules and RO membrane [23]. Thereby the increased in feed concentration caused the pH decreased as a result of the Donnan effect.

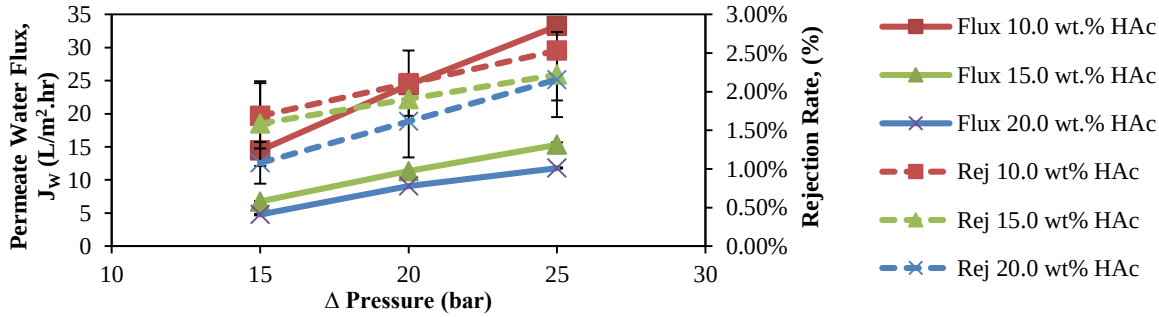

Figure 4 Effect of pressure on permeate of water flux and rejection rate at various feed concentration of membrane PSf 17.5 wt%

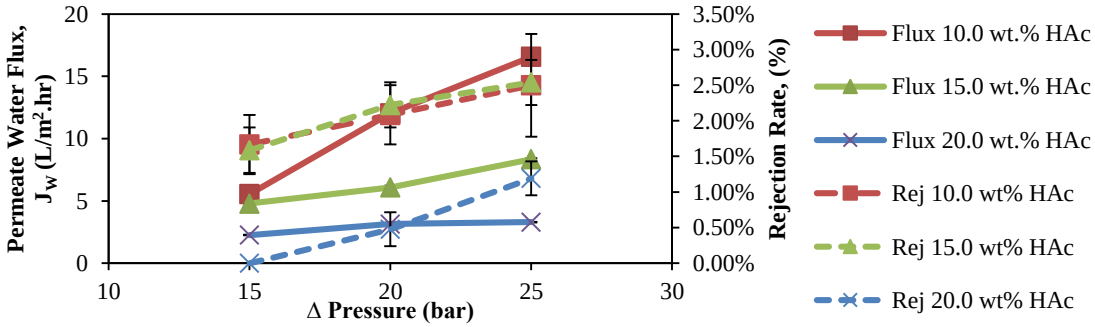

Figure 5 Effect of pressure on permeate of water flux and rejection rate at various feed concentration of membrane PSf 20.0 wt%

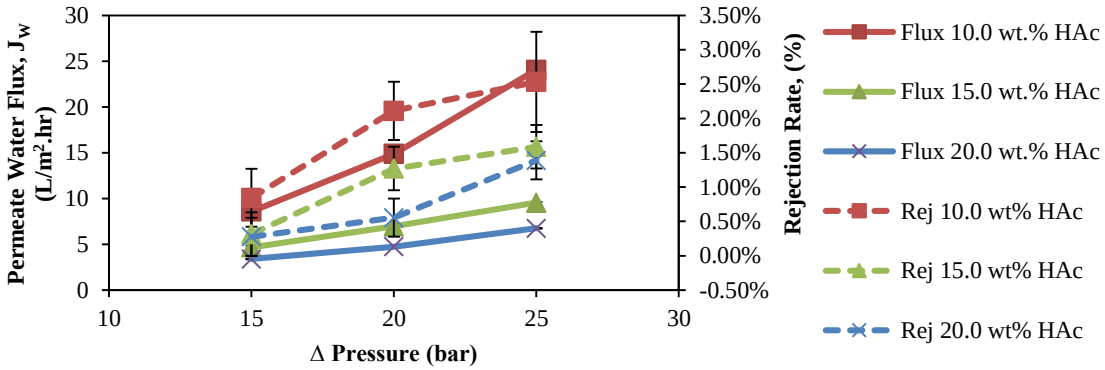

Figure 6 Effect of pressure on permeate of water flux and rejection rate at various feed concentration of membrane PSf (M) 17.5 wt%

3.5 Osmotic Pressure to Solute Concentration Ratio

Figure 7 to 10 show the relationship between the osmotic pressure to the solute concentration ratio of each membrane. The osmotic pressure is the minimum pressure that needs to be applied to a concentrated solution where the directions of water flow pass through the semi-permeable membrane was reversed. In general, the commercial AG membrane showed the lowest osmotic pressure for all HAc concentrations; 10.0 wt% HAc (15.41 m^2/h^2); 15.0 wt% HAc (17.18 m^2/h^2); and 20.0 wt% HAc (16.08 m^2/h^2). This osmotic pressure was overcome by the applied pressure (15, 20, 25 bar) to the acetic acid concentration, therefore the AG membrane showed the highest rejection rate as discussed in previous sections. For the synthesized membrane 17.5 wt% PSf, 20.0 wt% PSf and 17.5 wt% PSf (M), the overall osmotic pressures were more than 33.64 m^2/h^2 for all the HAc feed concentration. These results were coupled with a low rejection rate for all the synthesized membrane compared to commercial AG membrane.

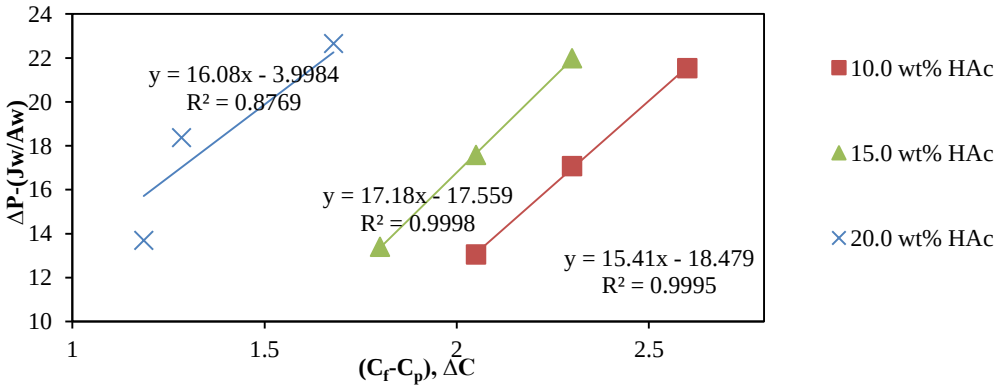

Figure 7 Osmotic pressure to solute concentration ratio of membrane AG

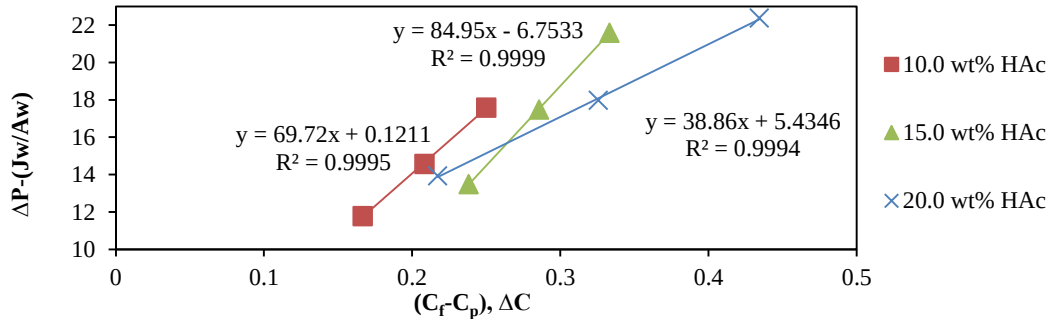

Figure 8 Osmotic pressure to solute concentration ratio of membrane PSf 17.5 wt%

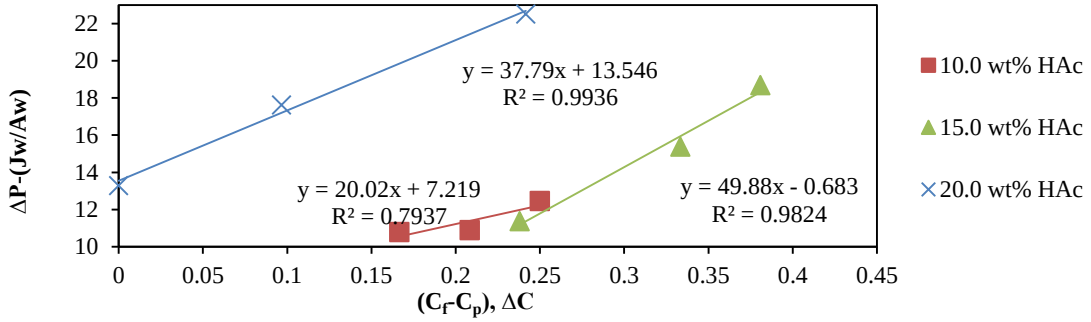

Figure 9 Osmotic pressure to solute concentration ratio of membrane PSf 20.0 wt%

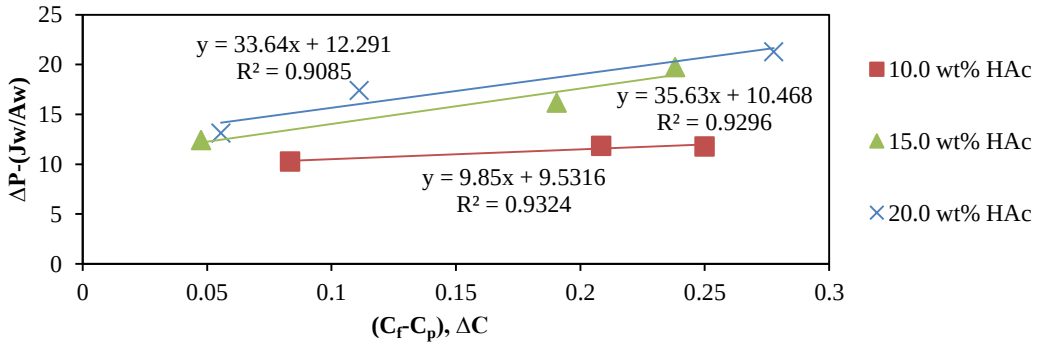

Figure 10 Osmotic pressure to solute concentration ratio of membrane PSf (M) 17.5 wt%

Table 2 is a summary of the osmotic pressure in different HAc concentration in the feed stream of different membrane. As can be seen in Table 2, when the HAc concentration increases the osmotic pressure also increases for all the membrane. However the osmotic pressure decreased consistently when the concentration of HAc increased from 15.0 wt% to 20.0 wt% for all type of membranes used. This occurrence is somehow beyond authors' comprehension. When the modified 17.5 wt% PSf membrane was applied, the osmotic pressure decreased. However, the value was still higher than that of the AG membrane. In Table 2, it summarises and compares the osmotic pressure of all the tested membranes. These results also indicate that the AG membrane has the highest rejection rate among all the membranes used.

Table 2 The results of osmotic pressure to solute concentration ratio

Type of membrane	osmotic pressure to solute concentration ratio, Ψ (m^2/h^2)		
	HAc 10.0 wt%	**HAc15.0 wt%**	**HAc 20.0 wt%**
AG	15.41	17.18	16.08
PSf 17.5 wt%	69.72	84.95	38.86
PSf 20.0 wt%	20.02	49.88	37.79
PSf (M) 17.5 wt%	9.85	35.63	33.64

3.2 Membrane Characterization

3.2 Membrane Morphological Study using FESEM

FESEM was employed to investigate both the top surface and cross-section morphologies of the membranes were presented in Figure 11 and 12 respectively. The images of the top surfaces of the membranes showed a significant difference (Figure 11 A, B, C, D). The 17.5 wt% PSf and 20.0 wt% PSf show that the top surface is very smooth compare to interfacial polyamide membrane AG and 17.5 wt% PSf (M) surfaces was rougher. Besides that, the interfacial membrane structure which consist of packed globules and a network of polymer strands. These features of interfacial polyamide membrane were persistent with the cross-linked polyamide structure formed with TMC during interfacial reaction [25]. As can be seen, the surface of polyamide membrane 17.5 wt% PSf (M) shown the unevenly formation of interfacial reaction compare to AG membrane.

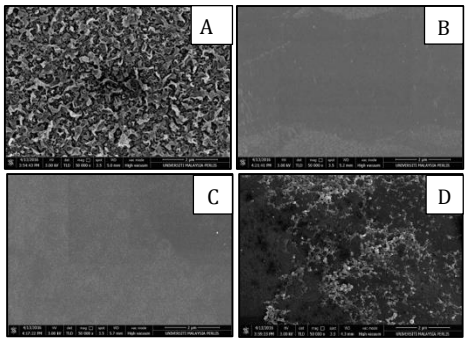

Figure 1 FESEM photograph (2 µm length scale and 50,000x magnification) of the top skin layer surface of the membrane: (A) AG; (B) 17.5 wt% PSf; (C) 20.0 wt% PSf; (D) 17.5 wt% PSf (M)

The cross-sectional images of the membranes were taken to study the effect of polymer concentration and modification towards membrane morphology. The cross-section images of Figure 12 (A-D focus on the PSf-based membrane; 17.5 wt% PSf, 20.0 wt% PSf and 17.5 wt% PSf (M) shows finger like structure of the membrane. The finger like structure of membrane 17.5 wt% PSf and 20.0 wt% PSf having the diameter around 9 µm and 15 µm and length about 51 µm and 105 µm respectively. In the SEM images of 17.5 wt% PSf membrane, it shows the macropores were resemblance to finger like structure. The images (Figure 12 A1, D1) represent the cross section of top layer of each membrane with the magnification of 35,000x, these images clearly show that the AG and 17.5 wt% PSf (M) membrane consists of thin

polyamide layer on top of the polysulfone support layers. The macrovoid structure of the polysulfone sublayer of the AG membrane appeared to begin right underneath the thin top layer where the interfacial reaction probably occurred [25].

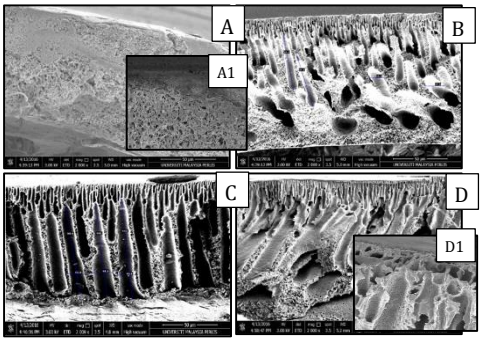

Figure 22 FESEM photograph (50 um length scale and 2,000x magnification) of the cross-sectional of the membrane: (A) AG; (B) PSf 17.5 wt%; (C) PSf 20.0 wt%; (D) PSf (M) 17.5 wt% and (3 um length scale and 35,000x magnification) of the top cross section of the membrane inset: (A1) AG; (D1) 17.5 wt% PSf (M)

From this observation, it was suggested that in order to increase the performance of the synthesized membrane, the finger-like pores in the membrane should be reduced and a homogenous thin PA layer is vital for excellence separation.

3.2.2. Fourier Transforms Infrared Spectroscopy (FTIR) Analysis

The purpose of Fourier Transform Infrared Spectroscopy (FTIR) is to analyse the presence of functional groups present on the skin layer surface of the membrane. The spectra were presented in two parts, which were the polysulfone sublayer and the polyamide layer which shown in Figure 12 and Figure 13 respectively. As can be seen from Figure 12 the spectra of the polysulfone sublayer of all membrane shows high peak at 2973 cm^{-1} which is associated with the C–H stretching of the methyl groups [26]. The strong reflectance in 1584–1487 is related with C–C stretching mode of aromatic ring. According to Tarboush *et al*., (2008) the band appears at 1295 cm^{-1} is the symmetric SO_2 stretching vibration, while the peak at 1150 cm^{-1}, 1105 cm^{-1} is the asymmetric SO_2 stretching vibration, the asymmetric C–O–C stretching frequencies which occur at 1240 cm^{-1}. These observations also are in accordance of the work by Jiang *et al*., (2006).

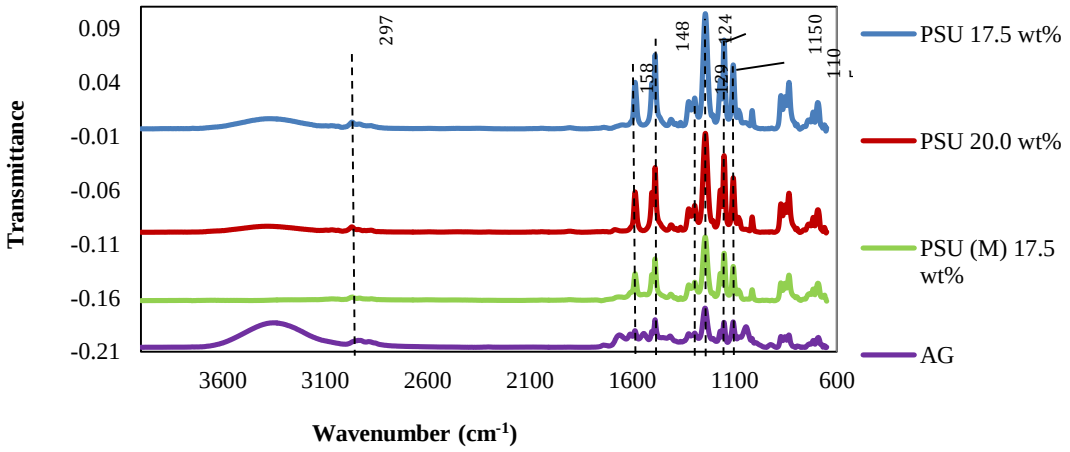

Figure 23 FTIR spectra of PSf peak in different membrane

On the other hand, the new peak was appeared in the polyamide layer which shown in Figure 14. Instead of peak polysulfone, the new absorption band which appeared at polyamide membrane AG is 3372 cm^{-1}, 1668 cm^{-1} and 1614 cm^{-1}, which can be assigned to O–H (and N–H) stretching, C=O bending of amide and N–H stretching of amide of mPA, while the peak at 1548 cm^{-1} is the C–N stretching of amide, these results can confirm the full coverage of the surface mPA [27]. The adsorption band at 1421 cm^{-1} can be confirmed the presence of C=O, O–H bending for carboxylic acid. Besides that for the membrane PSf (M) 17.5 wt% which have also done for the interfacial polymerisation, but the peak was only found at 1664 cm^{-1} and 1521 cm^{-1} which can assigned to C=O bending of amide and C–N stretching of amide. The incompletely of the polyamide absorption band in PSf (M) 17.5 wt %, resulted in unevenly coverage of MPD on the membrane surface. This result was shows the PSf (M) 17.5 wt% have almost same rejection rate as the membrane before modified (PSf 17.5 wt%) as discussed previously.

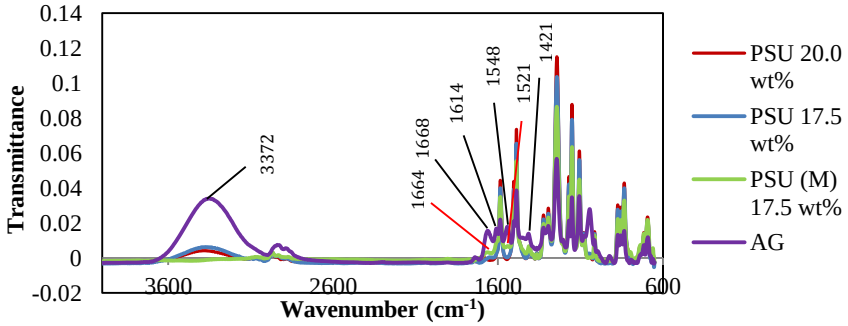

Figure 34 FTIR spectra of polyamide peak in different membrane

4.0 CONCLUSION

In this study, the commercial AG membrane and the synthesized polysulfone-based membranes were successfully fabricated using phase inversion-immersion precipitation method. All membranes were employed to separate HAc and water from dilute HAc mixture from the waste stream using a dead end filtration unit. The membrane performance was compared in terms of the permeate water flux, rejection rate of acetic acid and the osmotic pressure to solute concentration ratio. Variations of filtration conditions such as pressure and feed concentration on the membrane performance were also examined. For 10.0 wt% HAc, the commercial AG membrane shows the highest rejection rate among all the membrane applied with 26% rejection was recorded as the highest value. When the HAc concentration in the feed solution is increased to 20.0 wt% HAc, the rejection rate decreased to as low as 6% at 15 bar. For the synthesized membranes, the rejection rates were lower than that of the commercial AG membrane. In this study, the Donnan effect was not been evaluated in detail. From the literature, it was found that Donnan effect can cause the electrostatic interaction between charged solutes or molecules and membrane. The highest water flux was discovers in this study which was 17.5 wt% PSf membrane; the flux increased as pressure is increased. The result of osmotic pressure to solute concentration ratio showed that the commercial AG membrane has the lowest osmotic pressure in all HAc concentration compared to the other membranes. The membrane morphology was study using FESEM which indicates the membrane

morphology with top and cross sectional area of the thin film polyamide membrane. The FTIR study has assisted in identifying the membrane surface functional group of polysulfone and polyamide layer. The polysulfone groups were detected at wavenumber of 1295 cm^{-1}, 1150 cm^{-1} and 1105 cm^{-1} represents SO_2 symmetric and asymmetric stretching while polyamide layer were observes as 3372 cm^{-1}, 1668 cm^{-1} and 1614 cm^{-1} which assigned to to O–H (and N–H) stretching, C=O bending of amide and N–H stretching of amide of mPA. The result shows that the membrane with thin film polyamide which have the better rejection rate.

ACKNOWLEDGMENT

The authors would like to acknowledge the support from the Malaysian Ministry of Higher Education under a grant number of FRGS/1/2018/TK10/UNIMAP/02/2.

REFERENCES

[1] V. Ragaini, C. Pirola, A. Elli. 2005. Separation of Some Light Monocarboxylic Acids from Water Inbinary Solutions in a Reverse Osmosis Pilot Plant. *Desalination.* 171: 21-32.

[2] Malveda, M. 2007. Acetic acid (No. CEH Report 602.5000): SRI International.

[3] Z. Shen, J. Zhou, X. Zhou, Y. Zhang. 2011. The Production of Acetic Acid from Microalgae Under Hydrothermal Conditions. *Appl. Energy.* 88: 3444-3447.

[4] A. Vertova, G. Aricci, S. Rondinini, R. Miglio, L. Carnelli, P. D'Olimpio. 2009. Electrodialytic Recovery of Light Carboxylic Acids from Industrial Aqueous Wastes. *J. Appl. Electrochem*. 39: 2051-2059.

[5] V. Innocenzi, S. Zueva, M. Prisciandaro, I. De Michelis, A. Di Renzo, G. Mazziotti, F. Vegliò. 2019. Journal of Water Process Engineering Treatment of TMAH Solutions from the Microelectronics Industry : A Combined Process Scheme. *J. Water Process Eng.* 31: 100780.

[6] C. H. Shin, J. Y. Kim, J. Y. Kim, H. S. Kim, H. S. Lee, D. Mohapatra, J. W. Ahn, J. G. Ahn, W. Bae. 2009. A Solvent Extraction Approach to Recover Acetic Acid from Mixed Waste Acids Produced During Semiconductor Wafer Process. *J. Hazard. Mater.* 162: 1278-1284.

[7] C. Ni, X. Wu, J. Dan, D. Du. 2014. Facile Recovery of Acetic Acid from Waste Acids of Electronic Industry via a Partial Neutralization Pretreatment (PNP)-Distillation Strategy. *Sep. Purif. Technol.* 132: 23-26.

[8] Z. Lei, C. Li, Y. Li, B. Chen. 2004. Separation of Acetic Acid and Water by Complex Extractive Distillation. *Sep. Purif. Technol.* 36: 131-138.

[9] M. R. Usman, S. N. Hussain, H. M. A. Asghar, H. Sattar, A. Ijaz. 2011. Liquid-liquid Extraction of Acetic Acid from an Aqueous Aolution Using a Laboratory Scale Sonicator. *Journal of Quality and Technology Management.* 7(2): 115-121.

[10] N. Kawabata, T. Yamazaki, S. Yasuda. 1980. Process for Recovering a Carboxylic Acid. 4-9.

[11] K. L. Wasewar. 2005. Separation of Lactic Acid: Recent Advances. *Chem. Biochem. Eng. Q.* 19: 159-172.

[12] N. IsIklan, O. SanlI. 2005. Separation Characteristics of Acetic Acid-water Mixtures by Pervaporation Using Poly (Vinyl Alcohol) Membranes Modified with Malic Acid. *Chem. Eng. Process.* 44: 1019-1027.

[13] Y. Zhao, C. Qiu, X. Li, A.

Vararattanavech, R. Wang, X. Hu, A. G. Fane, C. Y. Tang. 2012. Synthesis of Robust and High-Performance Aquaporin-based Biomimetic Membranes by Interfacial Polymerization-Membrane Preparation and RO Performance Characterization. *Journal of Membrane Science*. 424: 422-428.

[14] V. Vatanpour, M. Sheydaei, M. Esmaeili. 2017. Box-Behnken Design as a Systematic Approach to Inspect Correlation between Synthesis Conditions and Desalination Performance of TFC RO Membranes. *Desalination*. 420: 1-11.

[15] A. Rahimpour, M. Jahanshahi, N. Mortazavian, S.S. Madaeni, Y. Mansourpanah. 2010. Preparation and Characterization of Asymmetric Polyethersulfone and Thin-film Composite Polyamide Nanofiltration Membranes for Water Softening. *Appl. Surf. Sci.* 256: 1657-1663.

[16] A. Sotto, A. Rashed, R. X. Zhang, A. Martínez, L. Braken, P. Luis, B. Van der Bruggen. 2012. Improved Membrane Structures for Seawater Desalination by Studying the Influence of Sublayers. *Desalination*. 287: 317-325.

[17] B. Qi, J. Luo, X. Chen, X. Hang, Y. Wan. 2011. Separation of Furfural from Monosaccharides by Nanofiltration. *Bioresour. Technol*. 102: 7111-7118.

[18] J. Radjenović, M. Petrović, F. Ventura, D. Barceló. 2008. Rejection of Pharmaceuticals in Nanofiltration and Reverse Osmosis Membrane Drinking Water Treatment. *Water Res.* 42: 3601-3610.

[19] A. Teella, G. W. Huber, D. M. Ford. 2011. Separation of Acetic Acid from the Aqueous Fraction of Fast Pyrolysis Bio-oils Using Nanofiltration and Reverse Osmosis Membranes. *J. Memb. Sci*. 378: 495-502.

[20] G. S. Murthy, S. Sridhar, M. Shyam Sunder, B. Shankaraiah, M. Ramakrishna. 2005. Concentration of Xylose Reaction Liquor by Nanofiltration for the Production of Xylitol Sugar Alcohol. *Sep. Purif. Technol.* 44: 221-228.

[21] Y. H. Weng, H. J. Wei, T. Y. Tsai, W. H. Chen, T. Y. Wei, W. S. Hwang, C. P. Wang, C. P. Huang. 2009. Separation of Acetic Acid from Xylose by Nanofiltration. *Sep. Purif. Technol*. 67: 95-102.

[22] B. Van Der Bruggen, J. Schaep, D. Wilms, C. Vandecasteele. 1999. Influence of Molecular Size, Polarity and Charge on the Retention of Organic Molecules by Nanofiltration. *J. Memb. Sci.* 156: 29-41.

[23] F. Zhou, C. Wang, J. Wei. 2013. Simultaneous Acetic Acid Separation and Monosaccharide Concentration by Reverse Osmosis. *Bioresour. Technol.* 131: 349-356.

[24] G. Yi, X. Fan, X. Quan, H. Zhang, S. Chen, H. Yu. 2019. A pH-responsive PAA-grafted-CNT Intercalated RGO Membrane with Steady Separation Efficiency for Charged Contaminants Over a Wide pH Range. *Sep. Purif. Technol.* 215: 422-429.

[25] O. Akin, F. Temelli. 2011. Probing the Hydrophobicity of Commercial Reverse Osmosis Membranes Produced by Interfacial Polymerization Using Contact Angle, XPS, FTIR, FE-SEM and AFM. *Desalination*. 278: 387-396.

[26] L. Y. Jiang, T. S. Chung, S. Kulprathipanja. 2006. An Investigation to Revitalize the Separation Performance of Hollow Fibers with a Thin Mixed Matrix Composite Skin for Gas Separation, *J. Memb. Sci.* 276: 113-125.

[27] B. J. Abu Tarboush, D. Rana, T. Matsuura, H. A. Arafat, R. M.

Narbaitz. 2008. Preparation of Thin-film-composite Polyamide Membranes for Desalination Using Novel Hydrophilic Surface Modifying Macromolecules. *J. Memb. Sci.* 325: 166-175.